HHS Public Access

Author manuscript

Mater Chem Phys. Author manuscript; available in PMC 2016 June 15.

Published in final edited form as:

Mater Chem Phys. 2015 June 15; 160: 177–186. doi:10.1016/j.matchemphys.2015.04.022.

The effects of synthesis method on the physical and chemical properties of dextran coated iron oxide nanoparticles

Anastasia K. Hauser, **Ronita Mathias**, **Kimberly W. Anderson**, and **J. Zach Hilt***

Department of Chemical and Materials Engineering, University of Kentucky, Lexington, KY 40506 U.S.A.

Abstract

Iron oxide nanoparticles coated with dextran were synthesized via four variations on the co-precipitation method. The methods ranged from *in situ* formation of the nanoparticles within the dextran solution to the adsorption of dextran to the nanoparticle surface following nucleation and extensive washing. The timing of the addition of dextran into the reaction mixture was found to greatly influence the physical and chemical properties of the magnetic nanoparticles. Batches of dextran coated iron oxide nanoparticles were synthesized by each method in triplicate, and the nanoparticles were further crosslinked with epichlorohydrin. The properties of the nanoparticles such as size, percentage of dextran coating, stability in solution, crystallinity, and magnetic properties were evaluated. The simultaneous semi-two-step method injected the reducing agent and the dextran solution into the reaction vessel at the same time. This method resulted in the greatest batch-to-batch reproducibility of nanoparticle properties and the least variation in nanoparticles synthesized in the same batch. The two-step method resulted in the greatest variation of the characteristics examined between batches. The one-step method was synthesized with both five grams and one gram of dextran to investigate the effects of solution viscosity on the resulting nanoparticle characteristics. The one-step method with five grams of dextran resulted in nanoparticles with significantly smaller crystal sizes (5.4 ± 1.9 nm) and lower specific adsorption rate (SAR) values (138.4 ± 13.6 W/g) in an alternating magnetic field (58 kA/m, 292 kHz). However, this method resulted in nanoparticles that were very stable in PBS over 12 hours, which is most likely due to the greater dextran coating (60.0 ± 2.7 weight percent). For comparison, the simultaneous semi-two-step method generated nanoparticles 179.2 ± 18.3 nm in diameter (crystal size 12.1 ± 0.2 nm) containing 18.3 ± 1.2 weight percent dextran with a SAR value of 321.1 ± 137.3 W/g.

Keywords

Nanomaterials; magnetic materials; co-precipitation; characterization

* Contact Author: J. Zach Hilt Associate Professor of Chemical Engineering Department of Chemical and Materials Engineering University of Kentucky 177 F. Paul Anderson Tower Lexington, KY 40506-0046 Tel.: +1-859-257-9844 Fax: +1-859-323-1929 hilt@engr.uky.edu.

1. Introduction

Nanoparticle research has been driven by the need for new technological applications in data storage, biomedical sciences, drug delivery, and therapeutics. Iron oxide nanoparticles represent a class of materials with such applications and are very promising due to their potential biocompatibility and magnetic properties which can be used for magnetic resonance imaging, magnetically mediated hyperthermia, etc. [1, 2]. The magnetic differences of iron oxide nanoparticles compared to the bulk material are a consequence of inter and intra particle interactions. Additionally, when the iron oxide nanoparticles are of a single domain, they exhibit superparamagnetism by which they do not retain magnetization in the absence of an externally applied magnetic field [3].

While the increased surface-to-volume ratio is an attractive property of superparamagnetic iron oxide nanoparticles, it also leads to considerable difficulty as a result of the tendency of nanoparticles to aggregate to reduce their surface energy by forming strong magnetic dipole interactions between the particles [4]. Monodispersed particles with high magnetic saturation are required for many biological applications, so it is often of interest to functionalize the nanoparticles with a coating layer to prevent agglomeration [5]. The coating layer can also be designed to increase the circulation time and the biocompatibility of the nanoparticles for use as MRI contrast agents and magnetically mediated hyperthermia [6, 7]. Dextran is a biocompatible long chain hydrophilic polymer composed of glucose with mostly α-1, 6 glycoside linkages [8] that strongly physisorb to magnetite nanoparticles in alkaline solutions via non-covalent interactions of the abundant hydroxyl groups resulting in enmeshed nanoparticle cores [3]. The hydroxyl groups of dextran can then be easily crosslinked and functionalized with primary amines to attach various targeting ligands, peptides, or probes [9-12]. Functionalization with primary amines throughout the nanosctructure allows for increased loading capacity and the potential for attachment of multiple targeting ligands, imaging agents or therapeutics into one system [13].

Iron oxide nanoparticles can be synthesized by various methods including co-precipitation [14-16], microemulsion [17], thermal decomposition [12, 18-22], and mechanical synthesis [23, 24]. The co-precipitation method has traditionally been the most common method and is the primary method by which clinically approved iron oxide nanoparticles are synthesized [25]. Co-precipitation requires the reaction to be performed in an inert atmosphere to prevent oxidation of the Fe^{2+} ions and oxidation of magnetite nanoparticles to maghemite. The surface of magnetite nanoparticles will oxidize to maghemite in the presence of oxygen which reduces the magnetic saturation of the material [26]. The process of co-precipitation involves initial nucleation followed by slow growth as the solutes diffuse to the surface of the crystal [4]. Within the co-precipitation method, there are various procedures that alter parameters of the reaction in order to tune the properties of the iron oxide nanoparticles produced. Variables such as pH, temperature, reaction time, and iron ion ratios have been examined to determine their effects on the size, stability, and heating properties of the nanoparticles. Vayssieres *et al.* [27] varied the pH of the reaction solution between 8.5 and 12 and found that the resulting iron oxide nanoparticles became smaller as the solution increased in alkalinity. It was also determined that a minimum pH of 10-11 is required for

the nanoparticle size to remain stable over time. Murbe *et al.* [28] addressed the effect of reaction temperature on the physical and chemical properties of iron oxide nanoparticles showing that as the temperature at which initial nucleation occurred increased from 25 to 70°C, the nanoparticle size also increased from 16 to 39 nm. Additionally, the magnetic saturation of the nanoparticles increased from 76 to 88 emu/g. Frimpong *et al.* [16] addressed the effects of reaction temperature and staged reactions on the magnetic properties of citrate capped iron oxide nanoparticles, and they also found that as temperature increased, the nanoparticle crystal size also increased. The saturation magnetization was also influenced by the reaction temperature and method as the one-step method resulted in nanoparticles with a lower magnetic saturation value and decreased heating capabilities than the two-step reactions. A significant amount of research has been completed on dextran coated iron oxide nanoparticles, specifically on varying the molecular weight of the dextran. Xu *et al.* [29] formed iron oxide nanoparticles in the presence of dextran with a molecular weight of 20 or 40 kDa. The 40 kDa dextran resulted in a viscous reaction solution, so the 20 kDa nanoparticles were preferred. However, the magnetic saturation of the nanoparticles was lower than expected due to significant agglomeration of the nanoparticles and a wide range of hydrodynamic radii. Although the effects of reaction temperature, time, pH, and dextran molecular weight have been analyzed, the time and method of dextran addition into the reaction solution has not yet been evaluated. Therefore, this manuscript seeks to determine the effects of the timely addition of dextran to the reaction mixture on the physical and chemical properties of the dextran coated iron oxide nanoparticles.

It is desired to understand the effects of dextran on the properties of iron oxide nanoparticles in order to develop a protocol that results in consistent and desired properties. As depicted in Figure1, four co-precipitation methods were developed to synthesize dextran coated iron oxide nanoparticles which were further crosslinked with epichlorohydrin to increase the thermodynamic stability of the dextran on the surface of the nanoparticles [30]. The methods varied by the time of dextran addition to the reaction mixture: from *in situ* formation of the iron oxide nanoparticles to formation followed by extensive washing prior to dextran adsorption. Three batches of nanoparticles were synthesized via each method in order to address the variability within a single method as well as the differences between the methods. All other parameters such as pH, reaction temperature, and dextran molecular weight were kept constant among the methods. After synthesis, both the dextran coated and epichlorohydrin crosslinked nanoparticles were characterized for size, dextran weight percent, stability, crystallinity, and heating ability in the presence of an alternating magnetic field. Each of these properties is important to evaluate prior to *in vivo* studies should the nanoparticles be used for biological applications. It is also important to develop protocols for iron oxide nanoparticle synthesis that result in consistent properties of the nanoparticles such as desired size, stability in solution, crystallinity to allow for heating in an AMF as well as image contrast, and dextran coating to increase circulation and biocompatibility. This article addresses the development of a synthesis method that results in consistent and desirable properties of iron oxide nanoparticles.

2. Materials and Methods

2.1 Materials

Iron (III) chloride hexahydrate ($FeCl_3 \cdot 6H_2O$), iron (II) chloride ($FeCl_2 \cdot 4H_2O$), 9 – 11 kDa dextran, epichlorohydrin (ECH) were obtained from Sigma Aldrich (St. Louis, MO). Ammonium hydroxide (NH_4OH) was purchased from EMD Chemicals (Gibbstown, NJ). Phosphate buffered saline solution (PBS) (10X) was purchased from EMD Millipore (Billerica, MA). All materials were used as received.

2.2 Dextran coated iron oxide nanoparticle synthesis via two-step method

A modified one-pot co-precipitation method [16] was used to prepare dextran coated IONPs. $FeCl_3 \cdot 6H_2O$ and $FeCl_2.4H_2O$ were combined in a 2:1 molar ratio (2.2 grams and 0.8 grams, respectively) and dissolved in 40 mL deionized (DI) water and sealed in a three-neck flask under vigorous stirring and an inert nitrogen environment. 5 grams of dextran was solubilized in 20 mL of DI water. The solution was heated to 85 °C at which 5 mL of NH_4OH was added dropwise to the reaction vessel. The reaction was carried out for 1 hour at 85 °C. The particles were magnetically decanted and washed three times with DI water. The nanoparticles were then re-suspended in 45 mL DI water and added to a three next flask. The dextran solution was added to the reaction vessel and the vessel was purged with nitrogen. The nanoparticles and dextran solution were stirred vigorously at room temperature for 24 hours. After 24 hours, the nanoparticles were magnetically decanted and washed three times with DI water. Finally, the nanoparticles were dialyzed against DI water for 24 hours (100 kDa molecular weight cutoff) then probe sonicated for 10 minutes and centrifuged at 1000 rpm for 5 minutes to remove large agglomerates.

2.3 Dextran coated iron oxide nanoparticle synthesis via semi-two-step method

$FeCl_3 \cdot 6H_2O$ and $FeCl_2.4H_2O$ were combined in a 2:1 molar ratio (2.2 grams and 0.8 grams, respectively) and dissolved in 40 mL deionized (DI) water and sealed in a three-neck flask under vigorous stirring and an inert nitrogen environment. 5 grams of dextran was solubilized in 20 mL of DI water. The solution was heated to 85 °C at which 5 ml of NH_4OH was added dropwise to the reaction vessel. The dextran solution was then injected dropwise into the vessel. The reaction was carried out for 1 hour at 85 °C. The particles were magnetically decanted and washed three times with DI water. The nanoparticles were then re-suspended in DI water and dialyzed against DI water for 24 hours (100 kDa molecular weight cutoff). After dialysis, the nanoparticles were probe sonicated for 10 minutes and then centrifuged at 1000 rpm for 5 minutes to remove large agglomerates.

2.4 Dextran coated iron oxide nanoparticle synthesis via simultaneous semi-two-step method

$FeCl_3 \cdot 6H_2O$ and $FeCl_2.4H_2O$ were combined in a 2:1 molar ratio (2.2 grams and 0.8 grams, respectively) and dissolved in 40 mL deionized (DI) water and sealed in a three-neck flask under vigorous stirring and an inert nitrogen environment. 5 grams of dextran was solubilized in 20 mL of DI water. The reaction solution was heated to 85 °C at which 5 ml of NH_4OH was added to the dextran solution and the combined solution was injected

dropwise into the vessel. The reaction was carried out for 1 hour at 85 °C. The particles were magnetically decanted and washed three times with DI water. The nanoparticles were then re-suspended in DI water and dialyzed against DI water for 24 hours (100 kDa molecular weight cutoff). After dialysis, the nanoparticles were probe sonicated for 10 minutes and then centrifuged at 1000 rpm for 5 minutes to remove large agglomerates.

2.5 Dextran coated iron oxide nanoparticle synthesis via one-step method

$FeCl_3 \cdot 6H_2O$ and $FeCl_2.4H_2O$ were combined in a 2:1 molar ratio (2.2 grams and 0.8 grams, respectively) and dissolved in 25 mL deionized (DI) water and sealed in a three-neck flask under vigorous stirring and an inert nitrogen environment. Five grams of dextran or one gram of dextran was solubilized in 50 mL of DI water and added to the three-neck flask. The solution was heated to 85 °C at which 5 ml of NH_4OH was injected dropwise into the vessel. The reaction was carried out for 1 hour at 85 °C. The particles were magnetically decanted and washed three times with DI water and then dialyzed against DI water for 24 hours (100 kDa molecular weight cutoff). After dialysis, the nanoparticles were probe sonicated for 10 minutes and then centrifuged at 1000 rpm for 5 minutes to remove large agglomerates.

2.6 Epichlorohydrin crosslinking of dextran coated iron oxide nanoparticles

Dextran coated IONPs were crosslinked using ECH for increased stability [30]. The particle colloid (9 mL, 1 mmol Fe) was added to 9 mL 5M NaOH and 1.5 mL ECH. The reaction was carried out for 24 hours at room temperature under continuous agitation. The particles were then magnetically decanted and dialyzed against DI water (100 kDa molecular weight cutoff) for 24 hours to remove excess ECH.

2.7 Particle characterization

Dynamic light scattering (DLS)—DLS measurements were obtained using a Beckman Coulter Delsa Nano C particle analyzer. Nanoparticle solutions were diluted to 200 μg/mL and were sonicated in a water bath prior to size analysis.

Ultraviolet (UV)-Visible spectroscopy—The stability of the nanoparticles was analyzed using a CaryWin 50 probe UV-visible spectrophotometer. IONPs were diluted to 200 μg/mL Fe in PBS. Sample absorbance was read at 540 nm over 12 hours.

Fourier transform infrared (FTIR) spectra—Attenuated total reflectance FTIR (ATR-FTIR) was used to determine surface functionalization with a Varian Inc. 7000e spectrometer. Dried samples were placed on the diamond ATR crystal and the spectrum was obtained between 700 and 4000 cm^{-1} for 32 scans.

Thermogravimetric analysis (TGA)—TGA was used to quantify the mass percent of the iron oxide core in the particle systems using a Netzsch Instruments STA 449A system. Approximately 5 mg of particle sample was heated at a rate of 5 °/minute. At 100 °C, the sample was held isothermally for 20 minutes to vaporize residual water. The samples were heated at 5 °/minute until reaching 500 °C where they were held isothermally for an additional 20 minutes. The reported mass loss was the actual mass loss normalized to the initial sample mass after isothermal heating at 100 °C.

Transmission electron microscopy (TEM)—TEM was completed using a JEOL 2010F system operating at 200 keV. IONPs were diluted to 1 mg/ml Fe in DI water and then dried on carbon TEM grids prior to analysis.

X-ray diffraction (XRD)—XRD patters were obtained by a Siemens D-500 X-ray spectrometer with a CuKα radiation source (λ = 1.54 Å) at 40 kV and 30 mA scanning from 5° to 65° at a scan rate of 1° per minute. The XRD patterns were used to confirm the magnetite crystal structure of the iron oxide nanoparticles. The XRD patterns are in coherence with JCPDS card (19-0629). The crystal domain size was estimated using the Scherrer equation [1]

$$\tau = \frac{K\lambda}{\beta cos\Theta} \quad [1]$$

where τ is the mean size of the ordered (crystalline) domains K is a dimensionless shape factor with a value close to unity(0.8396 for iron oxide) λ is the X-ray wavelength, β is the line broadening at half the maximum intensity (FWHM) after subtracting the instrumental line broadening, in radians and ϑ is the Bragg angle (17.72 °).

Alternating magnetic field (AMF) heating—The nanoparticle heating profiles were obtained using a custom made Taylor Winfield magnetic induction source, and the temperature was measured with a fiber optic temperature sensor (Luxtron FOT Lab Kit from LumaSense). Nanoparticle suspensions were diluted in DI water to a concentration of 3 mg/ml iron oxide. One milliliter of suspension in a 2 ml microcentrifuge tube was placed in the center of the AMF induction coil. The suspension was heated at a field amplitude of 58 kA/m and frequency of 292 kHz until the temperature of the suspension reached steady-state. The specific absorption rate (SAR) values of the nanoparticle suspensions were then calculated using the following equation:

$$SAR = \frac{C_{p,Fe} m_{Fe} + C_{p,H20} m_{H20}}{m_{Fe}} \frac{dT}{dt} \quad [2]$$

where $C_{p,Fe}$ is the heating capacity of iron, m_{Fe} is the mass of iron, $C_{p,H2O}$ is the heating capacity of water, m_{H2O} is the mass of water, and dT/dt is the initial slope of the heating profile. The intrinsic loss power (ILP) of the nanoparticle systems was calculated using the following equation:

$$ILP = \frac{SAR}{H^2 f} \quad [3]$$

where *H* is the magnetic field strength and *f* is the field frequency. This value will allow for the heating properties of these systems to be compared more accurately to other systems in literature.

3. Results and Discussion

The hydrodynamic diameter of the nanoparticles was analyzed via dynamic light scattering and reported as the z-average while the variability of particle size within the batches is quantified by the polydispersity index (PDI) in Table 1. The two-step method resulted in particles with the largest hydrodynamic diameter along with the greatest deviation between batches. The PDI of the nanoparticles synthesized by the two-step method was also the largest of the methods tested. After crosslinking with epichlorohydrin, the hydrodynamic diameter of the nanoparticles decreases significantly. This is likely due to the extra processing during crosslinking resulting in the loss of larger nanoparticle agglomerates. The one-step method with five grams of dextran resulted in the smallest nanoparticles most likely due to the high viscosity of the solution during nucleation inhibiting the transport of the iron ions to the nanoparticle surface. The high viscosity solution helps to prevent agglomeration of the nanoparticles but their formation is hindered due to transport limitations during the nucleation process. Although the one-step nanoparticles are smaller in hydrodynamic diameter which is advantageous for tumor targeting, their other properties such as heating abilities suffered from the high viscosity solution. The one-step method with one gram of dextran resulted in larger nanoparticles than the one-step method with five grams of dextran. Additionally, there is greater variability in the nanoparticle sizes between the batches. The simultaneous semi-two-step method resulted in nanoparticles with the most consistent sizes within a single batch as indicated by the low PDI after crosslinking, as well as the greatest batch to batch reproducibility as indicated by the lowest standard deviation. The batch-to-batch reproducibility is thought to be due to the simultaneous semi-two-step method being the easiest method to control since it involves a single injection of the ammonium hydroxide in a solution of dextran. The viscosity of the solution is also that of water when initial nucleation occurs allowing for iron ions to transport to the nucleation sites more effectively. Previous studies by Xu, et al. [29] found that lower molecular weight dextran (20kDa vs. 40kDa) was advantageous due to lower solution viscosity leading to more optimal nanoparticle characteristics. It is also important to note that low molecular weight dextran can precipitate acute renal failure so it is important to coat the nanoparticles with enough dextran to increase cytocompatibility and stability but not so much that excess dextran is administered [31]. In another study by Saraswathy et al. 70kDa dextran was used to coat iron oxide nanoparticles resulting in a 50 nm diameter and 12 nm core size. The high molecular weight dextran was offset by a using a low weight percentage dextran (3%) in water [32]. By using a high molecular weight dextran, the potential to cause osmotic nephropathy is decreased, but the amount of dextran coating the nanoparticle surface decreases, which could impact nanoparticle stability.

Different synthesis methods also have an effect on dextran adsorbed to the surface of the iron oxide nanoparticles. The presence of dextran on the surface of the iron oxide nanoparticles was confirmed via FTIR spectroscopy (Figure 2). The synthesis methods resulted in similar spectra with all spectra containing a broad peak between 3500-3200 cm^{-1} indicating the structural OH in the dextran chains. The peak associated with the asymmetrical stretching vibration of C-H in CH_2 is found at 2918 cm^{-1}. Peaks at 1450, 1350, and 1273 cm^{-1} can be assigned to the deformation vibration of H-C-OH of the dextran

chains. Finally, the asymmetrical and symmetrical vibrations of C-O-C can be found at 1157 and 849 cm^{-1}, respectively.

Quantification of the dextran coating was completed using thermogravimetric analysis (TGA) and is shown in Table 2. The one-step method with 5 grams of dextran resulted in the greatest dextran adsorption to the nanoparticle surface with approximately 60% of the nanoparticle weight being composed of dextran. On the contrary, the one-step method with one gram of dextran resulted in the least dextran adsorption and no significant change after crosslinking with epichlorohydrin as depicted in Figure 3e. The two-step method and the semi-two-step method resulted in the most variability between batches in the amount of dextran coating. In the semi-two-step method, this is most likely due to the multiple injections of ammonium hydroxide and dextran and slight variability in timing. Again, the simultaneous semi-two-step resulted in the most consistent dextran adsorption. All of the weight loss profiles display a single drop in mass as temperature increases indicating a single layer of dextran or crosslinked dextran on the nanoparticle surface (Figure 3). Additionally, after crosslinking, the mass due to the coating decreases or remains the same most likely due to further dialysis after crosslinking. The right shift in the temperature at which the greatest mass loss occurs confirms that dextran has been crosslinked as more energy is required to break the covalent bonds prior to degrade the coating.

Stability of the nanoparticles in solution is very important if the nanoparticles are to be used for biological applications as agglomeration could lead to blockage of the circulatory system or lack of targeting ability to the tissue of interest. Therefore, the stability of the nanoparticles in phosphate buffered saline was analyzed over a 12 hour time period for both the dextran coated and crosslinked systems synthesized by each of the methods (Figure 4). Dextran coated iron oxide nanoparticles synthesized by the one-step method with 5 grams of dextran were the most stable both before and after epichlorohydrin crosslinking. This is due to the steric interactions of dextran with the surrounding medium. Since the one-step with 5 grams of dextran has the greatest amount of dextran on the surface, it is expected that these nanoparticles would also be the most stable. However, the two-step, semi-two-step, and the simultaneous semi-two-step, resulted in relatively stable nanoparticles in PBS after crosslinking.

The XRD patterns (Figure 5) of the iron oxide nanoparticles synthesized by each method are in coherence with JCPDS card (19-0629) associated with magnetite. The sharp peaks indicate a highly crystalline structure has been formed by each method. The broad peak at approximately 2Θ equal to 17° is due to the presence of dextran which is confirmed by the XRD pattern of dextran only (Figure 5f). This peak has the greatest intensity in the one-step method with five grams of dextran which also has the greatest weight percent of dextran. Slight shoulders are seen in the XRD patters of the other synthesis methods confirming the presence of dextran, but the lower intensity matches the data obtained via thermogravimetric analysis. The highest intensity peak at 2Θ equal to 35.44° corresponds to the (3 1 1) plane of the iron oxide crystal structure. This peak was used to calculate the crystal size of the nanoparticles using the Scherrer equation and these crystal sizes correspond well with the crystal sizes shown in TEM (Figure 6). Table 3 displays the calculated crystal sizes from XRD spectra and the Scherrer equation along with the crystal sizes from TEM while Figure

5 depicts the XRD patterns. All the crystal sizes of the iron oxide nanoparticles synthesized are much smaller than the reported hydrodynamic diameter. This is due to multiple crystals being encapsulated within the dextran coating. The crystal size of the nanoparticles synthesized via the one-step method with 5 grams of dextran was significantly smaller than the crystal sizes of the nanoparticles synthesized by the other methods as shown by both XRD (Figure 5d) and TEM (Figure 6d). This is thought to be due to the concentrated dextran during nucleation. TEM images show the crystal size of nanoparticles synthesized via the two-step and semi-two step are larger than the other methods, which is due to dextran addition taking place post nucleation. Previous work has shown that crystal growth is retarded by the chemisorption of poly(vinyl alcohol) to the surface of the particles when synthesized by a one-step method [5]. Work completed by Pardoe et al. [33] has shown that iron oxide nanoparticles coated with dextran are significantly smaller than the control uncoated nanoparticles. Additionally, the polymer chosen to coat the nanoparticles influences the crystal size of the particles. For example, nanoparticles coated with PVA resulted in larger crystals than dextran coated particles but both were smaller than uncoated nanoparticles [33]. A similar effect was observed by Bee *et al.* [34] in which iron oxide nanoparticle formation was prevented by either chelation of citrate ions with metal ions and therefore preventing nucleation or by adsorption of the citrate ions on the nuclei inhibiting growth of the nuclei. Without a high dextran concentration and therefore a lower viscosity reaction solution, the iron oxide crystals have diameters closer to the other synthesis methods. Once again, the two step method results in the most variability in crystal size while the simultaneous semi-two-step is the most consistent.

The crystalline structure of iron oxide nanoparticles enables heating in the presence of an alternating magnetic field via multiple possible loss mechanisms including Néel paramagnetic switching, friction losses from Brownian rotation, and hysteresis [35]. Table 4 summarizes the specific adsorption rates of the nanoparticles in the presence of an AMF (58 kA/m, 292 kHz) and the corresponding intrinsic loss power (ILP). The one-step method with five grams of dextran resulted in nanoparticles with the lowest SAR values which are again due to dextran chemisorption to the surface of the nanoparticles after nucleation [8]. The other methods had greater SAR values as well as increased variability. The increased SAR value is thought to be due to nanoparticle agglomeration which would allow for ferromagnetic contributions resulting in increased heating. The excess dextran coating on the one-step method with 5 grams of dextran could also form a “dead layer” which would reduce the total effective moment of the nanoparticles [33, 36]. Daou *et al.* [37] established a similar effect by synthesizing magnetite nanoparticles and showing that carboxylate coupling to the nanoparticle surface could induce spin canting at the surface and reduce the saturation magnetization of the nanoparticles. Additionally, this effect has been observed with citrate capped magnetite nanoparticles synthesized via the co-precipitation method in a one or two-step procedure [16]. The decrease in SAR value after crosslinking with epichlorohydrin is most likely an artifact of the nanoparticles becoming more stable in solution and the additional probe sonication after dialysis. The nanoparticles are not significantly agglomerating and therefore heating via ferromagnetic contributions in addition to Neel paramagnetic switching and Brownian rotation. The ILP of these systems ranges from 0.16 to 0.39 nHm^2/kg with the one-step (5 grams Dx) being the lowest and the semi-

two-step being the highest, but with the most variability. Kallamadil et al. compared the ILP of commercial ferrofluids of various hydrodynamic sizes and found that for hydrodynamic diameters ranging from 100 to 170 nm and crystal sizes of approximately 7 nm, the ILP varies between 0.15 and 0.35 nHm^2/kg [38]. Therefore, these systems have heating properties comparable to those commercially available even though the alternating magnetic field strength may be slightly higher than others have used [39, 40].

4. Conclusions

Overall, the simultaneous semi-two-step method of synthesizing dextran coated iron oxide nanoparticles was the most consistent method and had the greatest batch-to-batch reproducibility. The nanoparticles synthesized by this method were stable in PBS for 12 hours, had hydrodynamic diameters less than 200 nm, generated sufficient heat in the presence of an AMF, and exhibited crystallinity consistent with magnetite. All of these properties can be tuned to varying degrees by simply altering the timing of dextran addition to the reaction. The amount of dextran also alters the properties of the nanoparticles. The one-step reaction was completed with both one and five grams of dextran to evaluate these effects. It was found that the nanoparticles synthesized with five grams of dextran are more stable, adsorb a greater amount of dextran on their surfaces, and have smaller hydrated diameters than the nanoparticles synthesized with one gram of dextran. However, the poor heating properties and small crystal sizes suggested that the one-step method with 5 grams of dextran may not be the preferred method for synthesizing the nanoparticles.

The one-step method with 1 gram of dextran yielded nanoparticles with improved heating properties and larger crystal sizes but larger and more inconsistent hydrolyzed diameters and decreased stability. The semi-two step and two-step methods resulted in nanoparticles with inconsistent physicochemical properties batch-to-batch. The heating properties were improved compared to the one-step with 5 grams dextran, but the size was larger with greater polydispersity indices. Also, the stability in PBS was decreased. Therefore, the method by which the dextran coated iron oxide nanoparticles are synthesized greatly affects the physical and chemical properties of the nanoparticles and thus, it is critical that the co-precipitation method for the preparation of magnetic nanoparticles is carefully developed and controlled to get desired properties for specific applications.

5. Acknowledgements

The project described was partially supported by Grant Number R25CA153954 from the National Cancer Institute. The content is solely the responsibility of the authors and does not necessarily represent the official views of the National Cancer Institute or the National Institutes of Health. Additionally, this material is based upon work supported by the National Science Foundation Graduate Research Fellowship Program Grant No. DGE-1247392. Any opinions, findings, and conclusions or recommendations expressed in this material are those of the author(s) and do not necessarily reflect the views of the National Science Foundation.

References

1. Andrade AL, Souza DM, Pereira MC, Fabris JD, Domingues RZ. pH EFFECT ON THE SYNTHESIS OF MAGNETITE NANOPARTICLES BY THE CHEMICAL REDUCTION-PRECIPITATION METHOD. Quimica Nova. 2010; 33:524–7.

2. Frimpong RA, Hilt JZ. Magnetic nanoparticles in biomedicine: synthesis, functionalization and applications. Nanomedicine. 2010; 5:1401–14. [PubMed: 21128722]
3. Yoffe S, Leshuk T, Everett P, Gu F. Superparamagnetic Iron Oxide Nanoparticles (SPIONs): Synthesis and Surface Modification Techniques for use with MRI and Other Biomedical Applications. Curr Pharm Design. 2013; 19:493–509.
4. Easo SL, Mohanan PV. Dextran stabilized iron oxide nanoparticles: Synthesis, characterization and in vitro studies. Carbohydrate Polymers. 2013; 92:726–32. [PubMed: 23218360]
5. Mahmoudi M, Simchi A, Milani AS, Stroeve P. Cell toxicity of superparamagnetic iron oxide nanoparticles. Journal of Colloid and Interface Science. 2009; 336:510–8. [PubMed: 19476952]
6. Laurent S, Dutz S, Hafeli UO, Mahmoudi M. Magnetic fluid hyperthermia: Focus on superparamagnetic iron oxide nanoparticles. Advances in Colloid and Interface Science. 2011; 166:8–23. [PubMed: 21601820]
7. Saraswathy A, Nazeer SS, Jeevan M, Nimi N, Arumugam S, Harikrishnan VS, et al. Citrate coated iron oxide nanoparticles with enhanced relaxivity for in vivo magnetic resonance imaging of liver fibrosis. Colloids and Surfaces B-Biointerfaces. 2014; 117:216–24.
8. Sreeja V, Joy PA. Effect of inter-particle interactions on the magnetic properties of magnetite nanoparticles after coating with dextran. International Journal of Nanotechnology. 2011; 8:907–15.
9. Kruse AM, Meenach SA, Anderson KW, Hilt JZ. Synthesis and characterization of CREKA-conjugated iron oxide nanoparticles for hyperthermia applications. Acta Biomater. 2014; 10:2622–9. [PubMed: 24486913]
10. Park J-H, Von Malzahn G, Zhang L, Schwartz MP, Ruoslahti E, Bhatia SN, et al. Magnetic iron oxide nanoworms for tumor targeting and imaging. Adv Mater. 2008; 20:1630–5. [PubMed: 21687830]
11. Simberg D, Duza T, Park JH, Essler M, Pilch J, Zhang L, et al. Biomimetic amplification of nanoparticle homing to tumors. Proceedings of the National Academy of Sciences. 2007; 104:932–6.
12. Ayala V, Herrera AP, Latorre-Esteves M, Torres-Lugo M, Rinaldi C. Effect of surface charge on the colloidal stability and in vitro uptake of carboxymethyl dextran-coated iron oxide nanoparticles. Journal of Nanoparticle Research. 2013:15.
13. Tassa C, Shaw SY, Weissleder R. Dextran-Coated Iron Oxide Nanoparticles: A Versatile Platform for Targeted Molecular Imaging, Molecular Diagnostic, and Therapy. Accounts of Chemical Research. 2011; 44:842–52. [PubMed: 21661727]
14. Massart R. PREPARATION OF AQUEOUS MAGNETIC LIQUIDS IN ALKALINE AND ACIDIC MEDIA. Ieee Transactions on Magnetics. 1981; 17:1247–8.
15. Kang YS, Risbud S, Rabolt JF, Stroeve P. Synthesis and characterization of nanometer-size Fe3O4 and gamma-Fe2O3 particles. Chemistry of Materials. 1996; 8:2209.
16. Frimpong RA, Dou J, Pechan M, Hilt JZ. Enhancing remote controlled heating characteristics in hydrophilic magnetite nanoparticles via facile co-precipitation. Journal of Magnetism and Magnetic Materials. 2010; 322:326–31.
17. Lee Y, Lee J, Bae CJ, Park JG, Noh HJ, Park JH, et al. Large-scale synthesis of uniform and crystalline magnetite nanoparticles using reverse micelles as nanoreactors under reflux conditions. Advanced Functional Materials. 2005; 15:503–9.
18. Park J, An KJ, Hwang YS, Park JG, Noh HJ, Kim JY, et al. Ultra-large-scale syntheses of monodisperse nanocrystals. Nature Materials. 2004; 3:891–5.
19. Sun SH, Zeng H, Robinson DB, Raoux S, Rice PM, Wang SX, et al. Monodisperse MFe2O4 (M = Fe, Co, Mn) nanoparticles. Journal of the American Chemical Society. 2004; 126:273–9. [PubMed: 14709092]
20. Lee YT, Woo K, Choi KS. Preparation of water-dispersible and biocompatible iron oxide nanoparticles for MRI agent. Ieee Transactions on Nanotechnology. 2008; 7:111–4.
21. Sharapova VA, Uimin MA, Mysik AA, Ermakov AE. Heat Release in Magnetic Nanoparticles in AC Magnetic Fields. Physics of Metals and Metallography. 2010; 110:5–12.
22. Buyukhatipoglu K, Clyne AM. Controlled flame synthesis of alpha Fe2O3 and Fe3O4 nanoparticles: effect of flame configuration, flame temperature, and additive loading. Journal of Nanoparticle Research. 2010; 12:1495–508.

23. Janot R, Guerard D. One-step synthesis of maghemite nanometric powders by ball-milling. Journal of Alloys and Compounds. 2002; 333:302–7.
24. Arbain R, Othman M, Palaniandy S. Preparation of iron oxide nanoparticles by mechanical milling. Minerals Engineering. 2011; 24:1–9.
25. Qiao RR, Yang CH, Gao MY. Superparamagnetic iron oxide nanoparticles: from preparations to in vivo MRI applications. J Mater Chem. 2009; 19:6274–93.
26. Gupta AK, Gupta M. Synthesis and surface engineering of iron oxide nanoparticles for biomedical applications. Biomaterials. 2005; 26:3995–4021. [PubMed: 15626447]
27. Vayssieres L, Chaneac C, Tronc E, Jolivet JP. Size tailoring of magnetite particles formed by aqueous precipitation: An example of thermodynamic stability of nanometric oxide particles. Journal of Colloid and Interface Science. 1998; 205:205–12. [PubMed: 9735184]
28. Murbe J, Rechtenbach A, Topfer J. Synthesis and physical characterization of magnetite nanoparticles for biomedical applications. Materials Chemistry and Physics. 2008; 110:426–33.
29. Xu XQ, Shen H, Xu, Xu J, Li XJ, Xiong XM. Core-shell structure and magnetic properties of magnetite magnetic fluids stabilized with dextran. Applied Surface Science. 2005; 252:494–500.
30. Palmacci, S.; Josephson, L. Synthesis of polysaccharide covered superparamagnetic oxide colloids. Advanced Magnetics, Inc.; United States: 1993.
31. Feest TG. LOW-MOLECULAR WEIGHT DEXTRAN - A CONTINUING CAUSE OF ACUTE RENAL-FAILURE. British Medical Journal. 1976; 2:1300. [PubMed: 1000202]
32. Saraswathy A, Nazeer SS, Nimi N, Arumugam S, Shenoy SJ, Jayasree RS. Synthesis and characterization of dextran stabilized superparamagnetic iron oxide nanoparticles for in vivo MR imaging of liver fibrosis. Carbohydrate Polymers. 2014; 101:760–8. [PubMed: 24299836]
33. Pardoe H, Chua-anusorn W, St Pierre TG, Dobson J. Structural and magnetic properties of nanoscale iron oxide particles synthesized in the presence of dextran or polyvinyl alcohol. Journal of Magnetism and Magnetic Materials. 2001; 225:41–6.
34. Bee A, Massart R, Neveu S. SYNTHESIS OF VERY FINE MAGHEMITE PARTICLES. Journal of Magnetism and Magnetic Materials. 1995; 149:6–9.
35. Dennis CL, Jackson AJ, Borchers JA, Hoopes PJ, Strawbridge R, Foreman AR, et al. Nearly complete regression of tumors via collective behavior of magnetic nanoparticles in hyperthermia. Nanotechnology. 2009; 20:395103. [PubMed: 19726837]
36. Kodama RH. Magnetic nanoparticles. Journal of Magnetism and Magnetic Materials. 1999; 200:359–72.
37. Daou TJ, Greneche JM, Pourroy G, Buathong S, Derory A, Ulhaq-Bouillet C, et al. Coupling agent effect on magnetic properties of functionalized magnetite-based nanoparticles. Chemistry of Materials. 2008; 20:5869–75.
38. Kallumadil M, Tada M, Nakagawa T, Abe M, Southern P, Pankhurst QA. Suitability of commercial colloids for magnetic hyperthermia (vol 321, pg 1509, 2009). Journal of Magnetism and Magnetic Materials. 2009; 321:3650–1.
39. Hergt R, Hiergeist R, Hilger I, Kaiser WA, Lapatnikov Y, Margel S, et al. Maghemite nanoparticles with very high AC-losses for application in RF-magnetic hyperthermia. Journal of Magnetism and Magnetic Materials. 2004; 270:345–57.
40. Fortin JP, Wilhelm C, Servais J, Menager C, Bacri JC, Gazeau F. Size-sorted anionic iron oxide nanomagnets as colloidal mediators for magnetic hyperthermia. Journal of the American Chemical Society. 2007; 129:2628–35. [PubMed: 17266310]

Highlights

- IONPs coated with dextran were synthesized via co-precipitation method variations
- The synthesis method greatly affected the physical and chemical properties
- The simultaneous semi-two-step method was the most reproducible method
- The two-step method resulted in the greatest variation between batches
- The effects of solution viscosity was studied for the one-step method

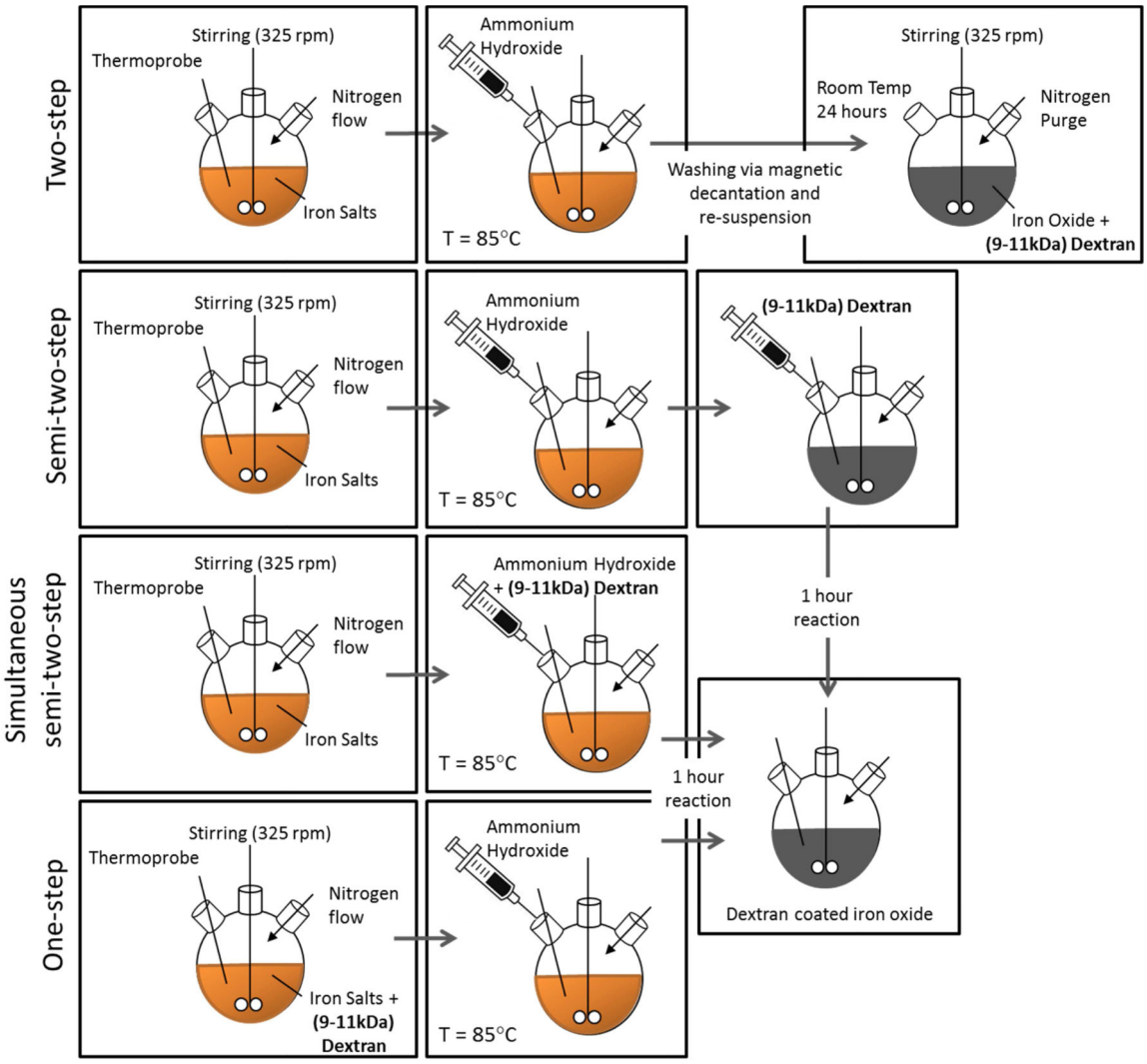

Figure 1.

Schematic of iron oxide nanoparticle synthesis methods. The co-precipitation reaction for each of the methods is completed at 85 °C for one hour after the addition of the reducing agent (ammonium hydroxide).

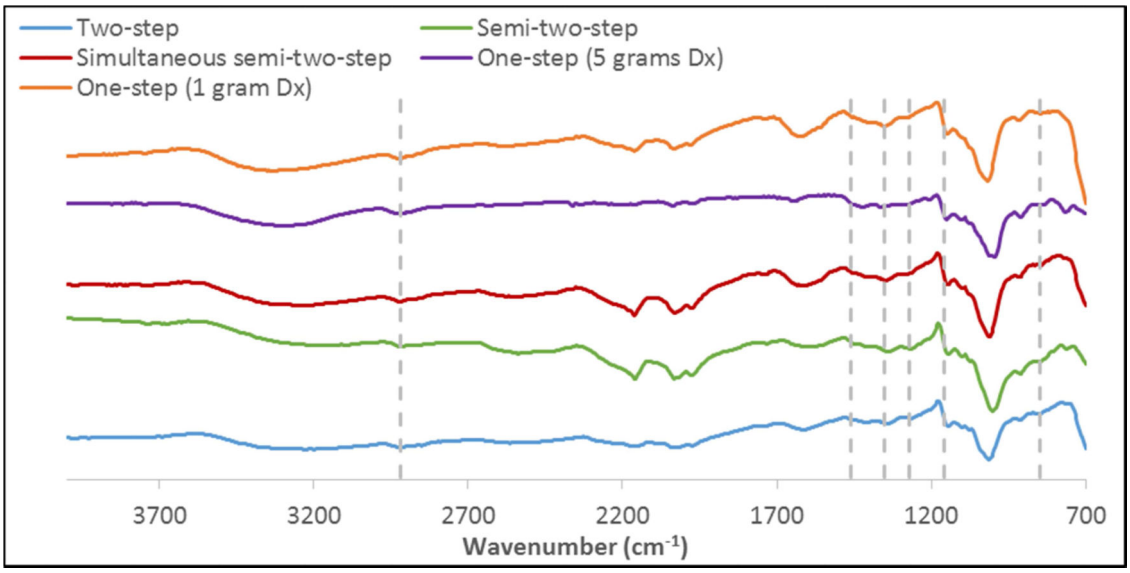

Figure 2.
FTIR spectra of dextran coated iron oxide nanoparticles synthesized by the various methods.

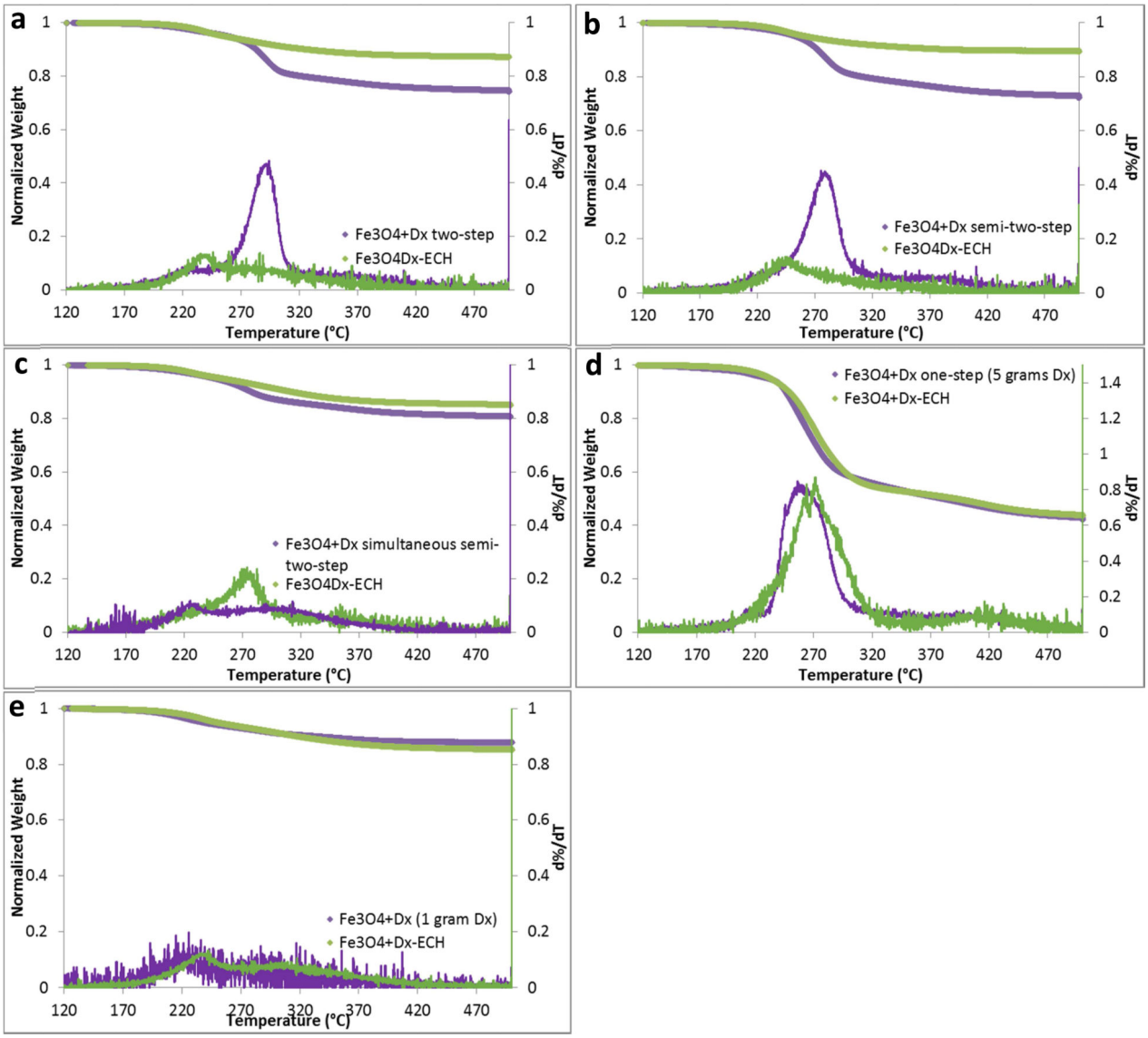

Figure 3.

Mass loss and d%/dT with increasing temperature of dextran coated and epichlorohydrin crosslinked iron oxide nanoparticles synthesized via the (a) two-step method, (b) semi-two-step method, (c) simultaneous semi-two-step method, (d) one-step method with 5 grams dextran, and (e) one-step method with 1 gram dextran.

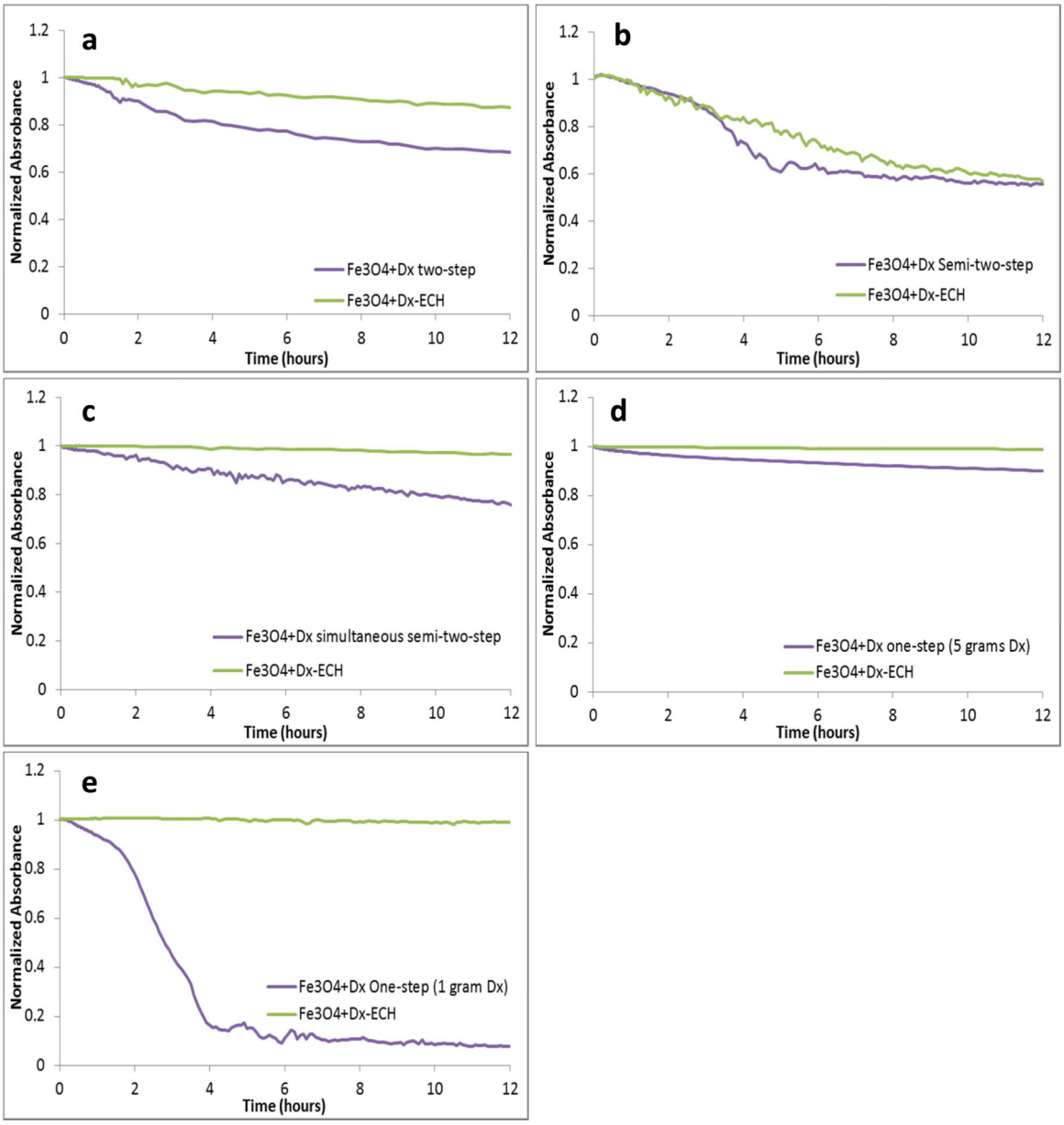

Figure 4.

Stability of dextran coated and epichlorohydrin crosslinked iron oxide nanoparticles synthesized via the (a) two-step method, (b) semi-two-step method, (c) simultaneous semi-two-step method, (d) one-step method with 5 grams dextran, and (e) one-step method with 1 gram dextran in PBS over 12 hours analyzed by UV-visible spectroscopy (λ=540).

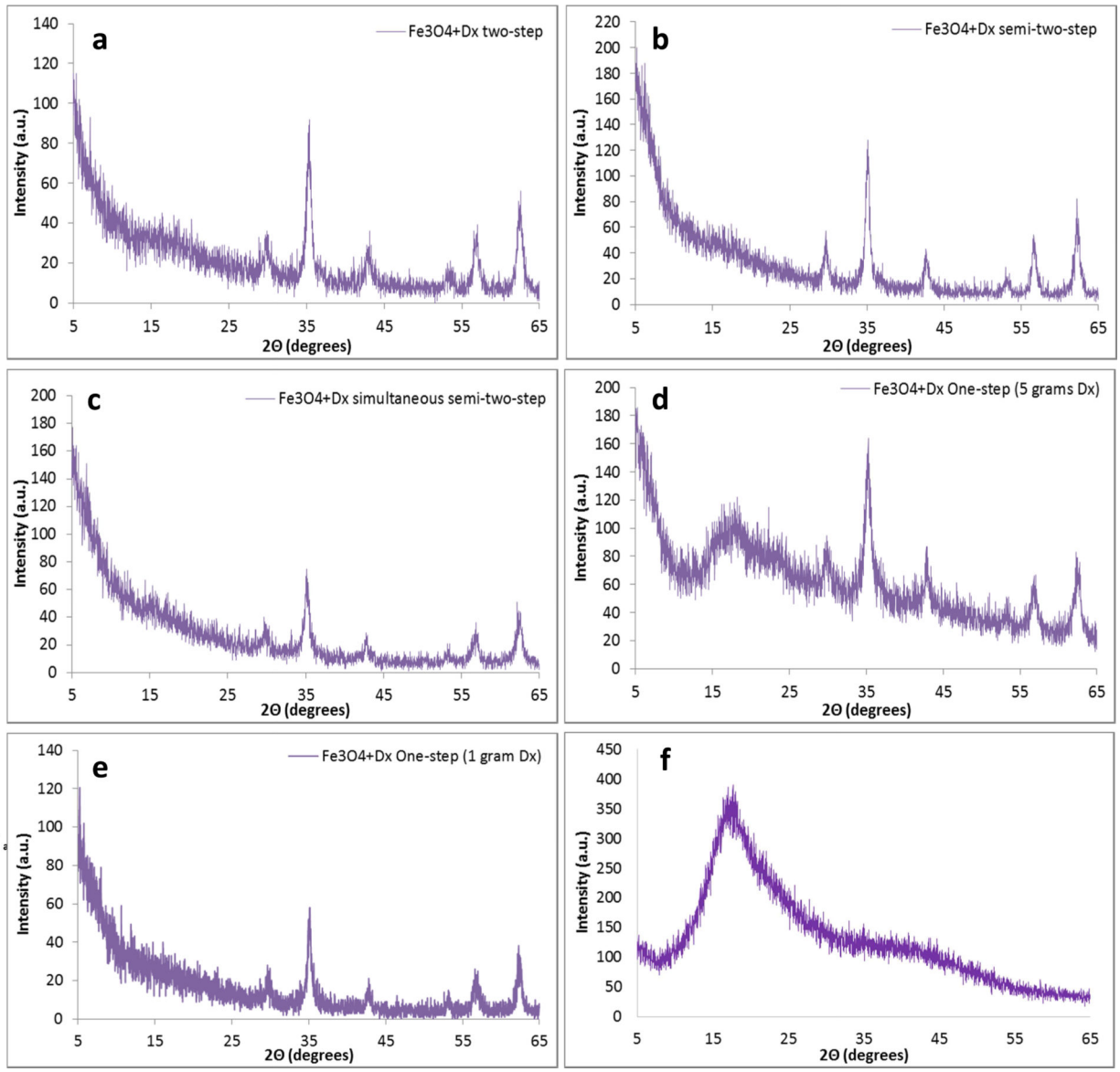

Figure 5.

XRD patters of dextran coated iron oxide nanoparticles synthesized via the (a) two-step method, (b) semi-two-step method, (c) simultaneous semi-two-step method, (d) one-step method with 5 grams dextran, (e) one-step method with 1 gram dextran and (f) dextran only.

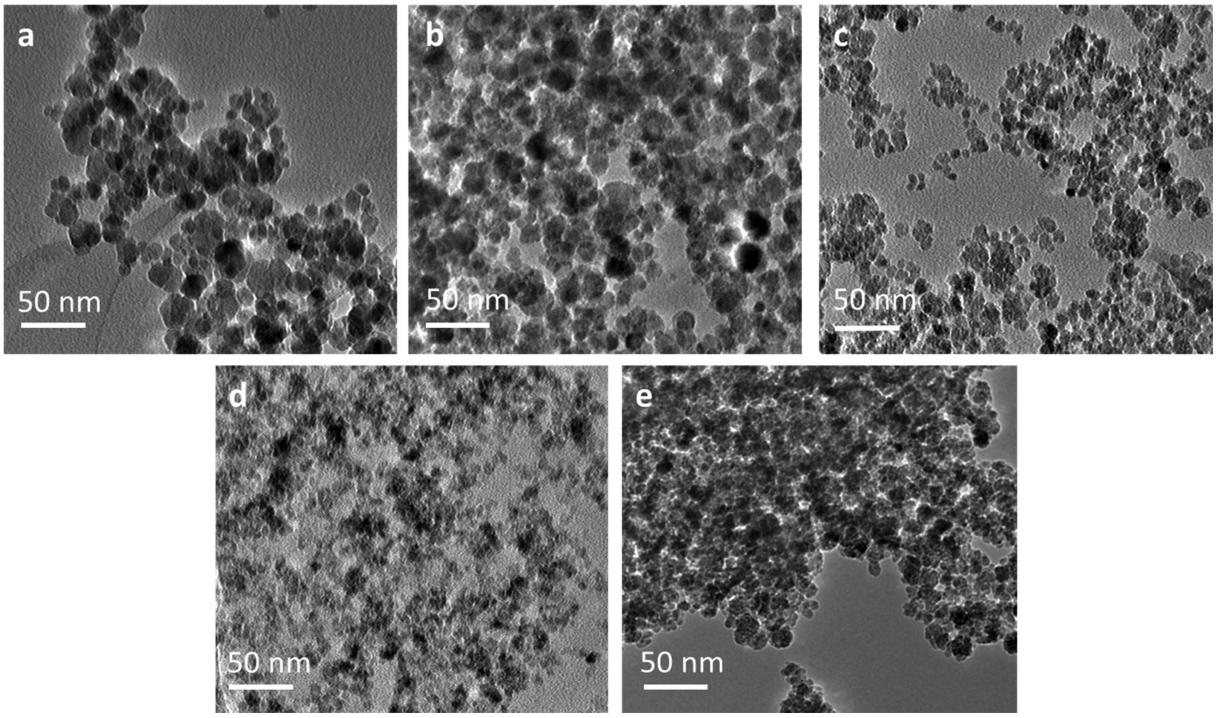

Figure 6.

TEM images of dextran coated iron oxide nanoparticles synthesized via the (a) two-step method, (b) semi-two-step method, (c) simultaneous semi-two-step method, (d) one-step method with grams dextran, and (e) one-step method with 1 gram dextran.

Table 1

Size analysis via dynamic light scattering of iron oxide nanoparticles synthesized by the various methods represented by average ± standard deviation (three independent batches and three samples from each batch).

Method	Nanoparticle	Size (nm)	PDI
two-step	Fe3O4+Dx	382.4 ± 163.2	0.35 ± 0.14
	Fe3O4+Dx-ECH	237.8 ± 28.8	0.16 ± 0.02
semi-two-step	Fe3O4+Dx	233.9 ± 25.2	0.19 ± 0.03
	Fe3O4+Dx-ECH	244.1 ± 54.7	0.20 ± 0.08
simultaneous semi-two-step	Fe3O4+Dx	179.2 ± 18.3	0.18 ± 0.02
	Fe3O4+Dx-ECH	185.6 ± 23.8	0.02 ± 0.03
one-step (5 grams Dx)	Fe3O4+Dx	171.4 ± 30.9	0.22 ± 0.09
	Fe3O4+Dx-ECH	121.7 ± 24.7	0.14 ± 0.02
one-step (1 gram Dx)	Fe3O4+Dx	248.0 ± 69.0	0.20 ± 0.05
	Fe3O4+Dx-ECH	244.2 ± 34.4	0.16 ± 0.05

Table 2

Dextran weight percentage via thermogravimetric analysis of iron oxide nanoparticles synthesized by the various methods (n=3).

Synthesis Method	Nanoparticle	Coating Weight%
two-step	Fe3O4+Dx	23.7 ± 7.8
	Fe3O4+Dx-ECH	19.0 ± 11.3
semi-two-step	Fe3O4+Dx	29.3 ± 6.1
	Fe3O4+Dx-ECH	16.7 ± 9.8
simultaneous semi-two-step	Fe3O4+Dx	18.3 ± 1.2
	Fe3O4+Dx-ECH	15.7 ± 5.0
one-step (5 grams Dx)	Fe3O4+Dx	60.0 ± 2.7
	Fe3O4+Dx-ECH	58.0 ± 7.2
one-step (1 gram Dx)	Fe3O4+Dx	12.7 ± 1.7
	Fe3O4+Dx-ECH	13.0 ± 1.7

Table 3

Iron oxide crystal size estimated using XRD spectra and the Scherrer equation and TEM images of iron oxide nanoparticles synthesized by the various methods (mean ± st. dev. n=3 for XRD and n=150 for TEM).

Synthesis Method	XRD Size (nm)	TEM Size (nm)
two-step	10.0 ± 2.1	14.5 ± 4.2
semi-two-step	11.2 ± 1.0	14.7 ± 4.6
simultaneous semi-two-step	12.1 ± 0.2	8.9 ± 2.2
one-step (5 grams Dx)	5.4 ± 1.9	6.8 ± 1.4
one-step (1 gram Dx)	12.4 ± 1.3	10.1 ± 3.1

Table 4

Specific absorption rates (W/g) of iron oxide nanoparticles (3 mg/mL Fe_3O_4) heating in an alternating magnetic field (58 kA/m, 292 kHz) of iron oxide nanoparticles synthesized by the various methods (n=3).

Method	Nanoparticle	SAR (W/g)	ILP (nHm^2/kg)
two-step	Fe3O4+Dx	323.6 ± 134.1	0.33 ± 0.14
	Fe3O4+Dx-ECH	297.6 ± 102.5	0.30 ± 0.10
semi-two-step	Fe3O4+Dx	384.3 ± 37.6	0.39 ± 0.04
	Fe3O4+Dx-ECH	313.4 ± 50.9	0.21 ± 0.05
simultaneous semi-two-step	Fe3O4+Dx	321.1 ± 137.3	0.33 ± 0.14
	Fe3O4+Dx-ECH	211.0 ± 46.6	0.21 ± 0.05
one-step (5 grams Dx)	Fe3O4+Dx	138.4 ± 13.6	0.14 ± 0.01
	Fe3O4+Dx-ECH	158.2 ± 51.1	0.16 ± 0.05
one-step (1 gram Dx)	Fe3O4+Dx	313.9 ± 42.1	0.32 ± 0.04
	Fe3O4+Dx-ECH	228.3 ± 32.4	0.23 ± 0.03